We are IntechOpen, the world's leading publisher of Open Access books Built by scientists, for scientists

6,900
Open access books available

186,000
International authors and editors

200M
Downloads

154
Countries delivered to

Our authors are among the

TOP 1%
most cited scientists

12.2%
Contributors from top 500 universities

WEB OF SCIENCE™

Selection of our books indexed in the Book Citation Index
in Web of Science™ Core Collection (BKCI)

Interested in publishing with us?
Contact book.department@intechopen.com

Chapter

Biomechanics of the Canine Elbow Joint

Thomas Rohwedder

Abstract

The canine elbow joint is a complex joint, whose musculoskeletal anatomy is well investigated. During the last 30 years kinematic analysis has gained importance in veterinary research and kinematics of the healthy and medial coronoid disease affected canine elbow joint are progressively investigated. Video-kinematographic analysis represents the most commonly used technique and multiple studies have investigated the range of motion, angular velocity, duration of swing and stance phase, stride length and other kinematic parameters, mostly in the sagittal plane only. However, this technique is more error-prone and data gained by video-kinematography represent the kinematics of the whole limb including the soft tissue envelope. A more precise evaluation of the in vivo bone and joint movement can only been achieved using fluoroscopic kinematography. Based on recent studies significant differences in the motion pattern between healthy joints and elbows with medial coronoid disease could be detected. Thereby not only adaptive changes, caused by pain and lameness, could be described, but primary changes in the micromotion of the joint forming bones could be found, which potentially represent new factors in the pathogenesis of medial coronoid disease. This chapter gives a review of current literature on elbow joint kinematics, with particular focus onto pathologic biomechanics in dysplastic canine elbows.

Keywords: elbow, elbow dysplasia, canine, biomechanics, kinematics, joint disease, medial coronoid disease, joint contact

1. Introduction

The canine elbow joint is a complex joint, whose musculoskeletal anatomy is well investigated. However, the in vivo function of the elbow joint, the individual movement of the humerus, radius and ulna relative to each other and the load distribution within the joint is still subject of present and future research. Especially pathophysiological motion of the elbow joint, leading to a mechanical overload of certain joint compartments, is not well understood and an interesting field of present veterinary research. Canine developmental elbow disease (DED), in particular medial coronoid disease (MCD), is one of the most common reasons for forelimb lameness in the dog and therefore this topic has not only academic, but also clinical relevance.

2. Anatomical basics

The canine elbow joint is composed of the humerus proximally and the radius and ulna distally, and can be divided into three joint compartments: the humero-ulnar, humero-radial and proximal radio-ulnar joint [1, 2]. The humero-ulnar joint is formed by the humeral trochlea and intercondylar region of the condyle and the ulnar trochlear notch, which extends from the anconeal process to the radial incisure, and continues to the medial coronoid process of the ulna. The humero-radial joint is formed by the capitulum of the humeral condyle and the radial head. The radial incisure and the medial aspect of the radial head form the proximal radio-ulnar joint. Altogether the elbow joint acts as a hinge joint (ginglymus) with extension and flexion being the main motion pattern and some amount of pronation and supination, mainly taken over by the radio-ulnar joint [1].

In healthy canine elbows the radio-ulnar joint shows a congruent shape without any step formation between the ulnar and radial joint surface, at least under static conditions. However, the humero-ulnar joint is not perfectly congruent even in healthy dogs [3–6]. The radii of curvature of the humeral condyle and ulnar trochlear notch show different values along their curvilinear course, resulting in reduced contact in the central notch region [3–7]. The trochlear notch shows a slightly elliptical shape, so that the anconeal process and distal aspect of the notch as well as the coronoid process are in contact with the humeral condyle. This kind of physiological humero-ulnar incongruence was first described in humans and could be detected in the canine elbow joint, too [4–6, 8, 9].

The maximum range of motion (ROM) varies between 110 to 150 degrees, with breed-specific maximum flexion of 25 to 49 degrees and maximum extension of 155 to 175 degrees [10–14]. The main extensor muscle of the elbow joint is the triceps brachii muscle [1]. Further this muscle prevents flexion of the elbow during the stance phase. The anconeal and tensor fasciae antebrachii muscles are additional extensors of the elbow joint. Flexion is performed by the biceps brachii and brachial muscles. The extensor carpi radialis muscle contributes to flexor function to some amount. The canine antebrachium can be pronated 17 to 50 degrees and supinated 31 to 70 degrees [10, 15]. The supinator and brachioradial muscles are responsible for supination of the antebrachium. The latter contributes only minimal to supination and is missing in some individuals [16]. The pronator teres and pronator quadratus muscles are responsible for pronation and the pronator teres muscle is supposed to contribute to elbow joint flexion as well [1, 2].

Four ligaments support the elbow joint: the medial and lateral collateral ligament, the annular ligament and interosseous ligament/interosseous membrane [1, 2]. The medial and lateral collateral ligaments origin from the medial and lateral humeral epicondyle. The medial collateral divides into two crura. The cranial one is weaker and attaches at the radius, while the stronger caudal one attaches mainly at the ulna and to some amount at the radius. The lateral collateral ligament consists of two crura as well. The cranial part attaches to the radius, and the caudal part attaches to the ulna and colligates with the annular ligament, which can contain a sesamoid bone [2]. The annular ligament runs transversely around the radial head spanning from the lateral to the medial aspect of the radial incisure of the ulna. It runs underneath the medial and lateral collateral ligaments. The radius and ulna are further attached to each other by the interosseous ligament and interosseous membrane, which spans the interosseous space. Distally the radius and ulna are connected to each other by the radioulnar ligament.

3. Elbow joint kinematics

3.1 Kinematic analysis

Kinematics describe the motion of body segments without measuring the forces acting onto that segments. Kinematic analysis allows evaluation of the range of motion, angular velocities, segmental velocities of each portion of the limb, stride frequency and stride length [17]. Depending on the technique used for the kinematic analysis, motion of bones and joints can be measured with a submillimeter accuracy [18–20].

Generally two forms of kinematic analysis can be differentiated: the video-kinematography, based on a video motion capture system, and the radiostereometric kinematic analysis (RSA), based on a radiographic system, coupled with high speed video cameras. Video motion capture kinematic systems use skin markers, attached to specific body areas, which are tracked in the generated videos of the moving animal and allow for calculation of the aforementioned parameters. Radiostereometric analysis can be marker based or performed without bone markers [21–30]. Furthermore, both kinematic analysis systems can be used to evaluate motion in the two or three dimensional (2D, 3D) space, depending on the technical setup [17].

The most commonly used technique is a video motion capture system based analysis. This technique is non-invasive and allows for evaluation of overall limb, limb segment or body segment motion. However, skin mounted markers do not match exactly the movement of the underlying bones. Movement of the soft tissues results in skin motion artifacts [21, 28, 31–35], with a difference of 0.4 to 1.2 cm between the skin marker and respective underlying bony landmark in small animals [33]. Especially in the proximal joints of the forelimb skin marker based data differ significantly from fluoroscopically gained kinematic data [28]. Comparison of biplanar fluoroscopy and video-kinematography in hindlimb kinematics revealed significant differences between both techniques, too [21]. Skin marker based data tend to project different trajectories and smaller amplitudes compared to fluoroscopic kinematography with particularly contradictory results, especially in proximal joints, where increased soft tissues can be found [21].

Radiostereometric analysis, also called fluoroscopic kinematography, allows for the most accurate kinematic data acquisition [19, 21–24, 28, 30]. One or two fluoroscopic units, coupled with high speed video cameras, take x-ray movies of the moving object. Based on these x-ray movies bone movement can be calculated and transferred onto 3D bone models generated from CT scans of the individual animal. Bone motion analysis can be performed using implanted bone markers, which are tracked in one (uniplanar, 2D evaluation) or both (biplanar, 3D evaluation) x-ray movies and 3D coordinates of each marker are then transferred onto the 3D bone models. Alternatively, scientific rotoscoping or autoscoping techniques can be used to track bone movement and transfer this in vivo bone motion from the fluoroscopic images onto 3D bone models [18, 20, 36]. These techniques do not rely on bone markers, rather the shape and edges of each bone are used to project digitally reconstructed radiographs (DRR), generated from the CT scans of each bone, onto the respective bone in the fluoroscopic image. By that the 3D bone model is aligned and animated along the x-ray movies. Scientific rotoscoping is performed manually, while autoscoping is a completely computerized process. Both techniques can be described as morphology based methods of motion analysis. Marker based tacking is the gold standard of kinematic analysis with an accuracy of 0.1 mm and 0.1 degrees [20].

However, scientific rotoscoping and autoscoping show a high accuracy as well, with values ranging from 0.16 to 0.66 mm in translation and 0.43 to 2.78 degrees rotation for scientific rotoscoping and 0.07 to 1.13 mm translation and 0.01 to 3.0 degrees rotation for autoscoping [18, 37–42]. Therefore, both techniques result in a highly precise evaluation of bone and joint motion with a substantially reduced invasiveness compared to a bone marker based analysis.

Multiple studies have investigated elbow joint kinematics in healthy dogs and dogs with different joint pathologies. Results have to be interpreted cautiously due to varying breeds, different technical setups and varying gaits and gait velocities, e.g. the walk or the trot, all of which influencing the kinematic pattern. **Table 1** gives an overview of previous studies on canine forelimb and elbow joint kinematics.

Study	Technique	Breed	Number of dogs	Gait/Speed
DeCamp et al. [43]	3D marker based video-kinematography, 2D evaluation (sagittal motion)	Greyhound	8	trot, 1.8–2.3 m/s (walkway)
Allen et al. [44]	3D marker based video-kinematography, 2D evaluation (sagittal motion)	Mixed breed dogs	14	trot, 1.8–2.3 m/s (overground)
Hottinger et al. [45]	3D marker based video-kinematography, 2D evaluation (sagittal motion)	Different large breed dogs	15	walk, 0.9–1.1. m/s (overground)
Gillette and Zebas [46]	Uniplanar marker based video-kinematography, 2D evaluation (sagittal motion)	Labrador Retriever	16	trot, 2.8 m/s
Nielsen et al. [47]	3D marker based video-kinematography, 2D evaluation (sagittal motion), stance phase only	Mixed breed dogs	6	walk, 0.8–1.0 m/s (overground)
Owen et al. [48]	Uniplanar marker based video-kinematography, 2D evaluation (sagittal motion)	Greyhound	11	trot, 2.2–2.4 m/s (treadmill)
Clements et al. [49]	Uniplanar marker based video-kinematography, 2D evaluation (sagittal motion)	Labrador Retriever	10	trot, 2.0 m/s (treadmill)
Feeney et al. [50]	Uniplanar marker based video-kinematography, 2D evaluation (sagittal motion)	Labrador Retriever	10	walk, velocity not documented (overground)
Burton et al. [51]	3D marker based video-kinematography, 2D evaluation (sagittal motion)	Different mid to large breed dogs	7 (unilateral elbow disease)	trot, velocity not documented (treadmill)

Study	Technique	Breed	Number of dogs	Gait/Speed
Holler et al. [52]	3D marker based video-kinematography, 2D evaluation (sagittal motion)	Different mid to large breed dogs	8	walk, 0.89–1.1 m/s (treadmill, normal, uphill, downhill, obstacle)
Agostinho et al. [53]	3D marker based video-kinematography, 2D evaluation (sagittal motion)	Labrador Retriever Rottweiler	20 (10 each)	trot, 2.1–2.2. m/s (treadmill)
Guillou et al. [54]	3D marker based fluoroscopic kinematography	Fox hound	4	walk & trot, velocity not documented
Angle et al. [55]	Uniplanar marker based video-kinematography, 2D evaluation (sagittal motion)	Greyhound	7	Movement initiation up to 3.52 m/s (overground)
Jarvis et al. [56]	3D marker based video-kinematography, 2D evaluation (sagittal motion), stance phase only	Different breeds	40 (24 healthy, 16 front limb amputee dogs)	trot, 2.2–2.6 m/s (walkway)
Brady et al. [57]	3D marker based video-kinematography, 2D evaluation (sagittal motion)	Different breeds	16	trot, 1.8 m/s & 2.5 m/s (walkway)
Miqueleto et al. [58]	3D marker based video-kinematography, 2D evaluation (sagittal motion)	German Shepherd	20 (10 hip dysplasia, 10 healthy dogs)	trot, 2.1–2.2. m/s (treadmill)
Galindo-Zamora et al. [59]	3D marker based video-kinematography, 2D evaluation (sagittal motion)	Different mid to large breed dogs	20 (unilateral elbow disease)	walk, 0.65–1.1 m/s (treadmill)
Caron et al. [60]	3D marker based video-kinematography, 3D evaluation	Labrador Retriever	26 (13 healthy, 13 dogs with coronoid disease)	walk, 0.7 m/s (treadmill)
Fischer & Lilje, [61]	3D marker based video- & fluoroscopic kinematography, 2D evaluation (sagittal motion)	32 different breeds	327	walk & trot, 0.54–5.56 m/s (treadmill)
Catavitello et al. [62]	Uniplanar marker based video-kinematography, 2D evaluation (sagittal motion)	Labrador Retriever Golden Retriever	6 (3 each breed)	walk, 2 m/s, trot, 4 m/s & running, 9.5 m/s (overground)
Duerr et al. [63]	Uniplanar marker based video-kinematography, 2D evaluation (sagittal motion) and inertial measurements unit	Different mid to large breed dogs	16	trot, 2.4–2.5 m/s (overground)

Study	Technique	Breed	Number of dogs	Gait/Speed
Andrada et al. [28]	3D marker based video- & fluoroscopic kinematography (scientific rotoscoping), 3D evaluation	Beagle	5	walk, 0.98 m/s & trot, 2.2 m/s (treadmill)
Lorke et al. [64]	3D marker based video-kinematography, 2D evaluation (sagittal motion)	Beagle	10	trot, 1.7–1.8 m/s (treadmill)
Rohwedder et al. [22]	3D marker based fluoroscopic kinematography (first third of stance phase only)	Different mid to large breed dogs	11 (5 healthy, 6 dogs with coronoid disease)	walk, 0.6–0.9 m/s (treadmill)
Kopec et al. [65]	Uniplanar marker based video-kinematography, 2D evaluation (sagittal motion)	Different mid to large breed dogs	8	walk, 1.01–1.45 m/s (overground & stair exercise)
Rohwedder et al. [23]	3D marker based fluoroscopic kinematography (first third of stance phase only)	Different mid to large breed dogs	11 (5 healthy, 6 dogs with coronoid disease)	walk, 0.6–0.9 m/s (treadmill)
Rohwedder et al. [24]	3D marker based fluoroscopic kinematography & joint contact pattern evaluation	Labrador Retriever	1 (before and after DPUO[*])	walk, 0.6–0.9 m/s (treadmill)
Humphries et al. [66]	3D marker based video-kinematography, 2D evaluation (sagittal motion)	Labrador Retriever German Shepherd	24 (12 each breed)	trot, 2.19–2.45 m/s (walkway)
De Souza et al. [67]	3D marker based video-kinematography, 2D evaluation (sagittal motion)	American Pit Bull Terrier	11	walk, 1.17 ± 0.17 m/s trot, 2.04 ± 0.33 m/s (overground)

[*]*DPUO: dynamic proximal ulnar osteotomy.*

Table 1.
Summary of studies investigating canine forelimb and/or elbow joint kinematics.

3.2 The healthy elbow joint

Most studies on elbow joint kinematics are based on video-kinematographic analysis and have investigated the motion of the elbow only in the sagittal plane [43–45, 47–53, 55–59, 62, 63, 65, 68, 69]. Caron et al. were the first to describe the real 3D kinematics of the canine forelimb of healthy Labrador retrievers and dogs with medial coronoid disease using video-kinematographic analysis [60]. Another study evaluated the 3D motion of orthopedic healthy canine forelimbs using video-kinematography and compared that data to fluoroscopically gained motion analysis, which was additionally calculated in one of the dogs [28].

One complete gait cycle consists of the swing and the stance phase. The swing phase starts when the paw breaks contact with the ground and ends with first ground

contact of the paw. The time between initial ground contact and paw lift is defined as the stance phase. The ratio between swing and stance phase depends from the gait pattern and the dog's velocity [28, 29, 70, 71]. At the walk the swing phase of the forelimb accounts for 39 to 43% of the whole gait cycle [60] and increases to approximately 50% to two thirds of the whole gait cycle during the trot, depending from the trotting speed [28, 43, 45, 58, 62, 64, 66]. During running the swing phase is further prolonged and accounts for approximately 75% of the gait cycle [62]. Conversely, with increasing speed the stance phase decreases [45, 70, 71].

The sagittal plane range of motion of the elbow joint (flexion-extension) is between 48.1 degrees and 70 degrees during one complete gait cycle when the dog is moving on a flat surface (**Table 2**), with the majority of motion occurring during the swing phase [28, 43–45, 47–50, 52, 53, 56–61, 63–67]. Range of motion is influenced by different parameters like breed, limb and body segment length, gait, velocity, exercise, age, contralateral limb amputation and concurrent orthopedic disease. With increasing speed of the gait the range of motion of joints increases [29, 45, 57, 62, 66, 68, 69]. Obese dogs show an increased range of motion as well, especially during the stance phase [57]. However, increasing age leads to an decrease in total range of motion, even in orthopedic healthy dogs [64]. Further, different exercises like descending stairs, uphill and downhill walking influence the range of motion, with descending stairs, obstacle exercises and uphill walking increasing the range of motion, while downhill walking decreases the amount of sagittal motion in the elbow [52, 65].

Study	Breed	Range of motion (°)	Flexion/Extension (°)	Gait/Speed
DeCamp et al. [43]	Greyhound	53.7	86.8/140.5	trot, 1.8–2.3 m/s (walkway)
Allen et al. [44]	Mixed breed dogs	55.8	93.7/149.5	trot, 1.8–2.3 m/s (overground)
Hottinger et al. [45]	Different large breed dogs	48.1	—	walk, 0.9–1.1. m/s (walkway)
Gillette and Zebas [46]	Labrador Retriever	right: 69.1 left: 66.1	—	trot, 2.8 m/s
Nielsen et al. [47]	Mixed breed dogs	—	111.7 ± 12/136.3 ± 10.4 (stance phase only)	walk, 0.8–1.0 m/s (overground)
Owen et al. [48]	Greyhound	49.35–49.59	100.98–102.7/150.57–152.05	trot, 2.2–2.4 m/s (treadmill)
Clements et al. [49]	Labrador Retriever	59.3 (SD 5.5)	—	trot, 2.0 m/s (treadmill)
Feeney et al. [50]	Labrador Retriever	54.8 ± 17.9	91.4/146.3	walk, velocity not documented(overground)
Holler et a. [52]	Different mid to large breed dogs	normal: 52.9 ± 7.0 uphill: 54.2 ± 7.4 downhill: 43.1 ± 5.8 obstacle: 57.0 ± 6.9	—	walk, 0.89–1.1 m/s (treadmill, normal, uphill, downhill, obstacle)

Study	Breed	Range of motion (°)	Flexion/Extension (°)	Gait/Speed
Agostinho et al. [53]	Labrador Retriever Rottweiler	63.77 ± 4.83 54.86 ± 5.16	90.52 ± 11.66/154.28 ± 9.64 93.99 ± 10.19/148.85 ± 9.15	trot, 2.1–2.2. m/s (treadmill)
Jarvis et al. [56]	Different breeds	stance phase only: control: 33.3 ± 8.6 amputee: 39.7 ± 10.4	control: 123.0 ± 12.9/ 156.4 ± 12.2 amputee: 119.2 ± 12.8/ 158.9 ± 12.5	trot, 2.2–2.6 m/s (walkway)
Brady et al. [57]	Different breeds	lean: 52.5 (1.8 m/s) obese: 65.0 (1.8 m/s) lean: 54.0 (2.5 m/s) obese: 62.0 (2.5 m/s)	lean: 95 ± 7/147 ± 17 obese: 90 ± 11/155 ± 9 lean: 93 ± 8/147 ± 9 obese: 88 ± 14/150 ± 18	trot, 1.8 m/s & 2.5 m/s (walkway)
Miqueleto et al. [58]	German Shepherd	healthy: 68.15 ± 7.19 hip dysplasia: 63.54 ± 13.53	healthy: 61.99/131.77 ± 7.60 hip dysplasia: 69.09/133.68 ± 11.37	trot, 2.1–2.2. m/s (treadmill)
Galindo-Zamora et al. [59]	Different mid to large breed dogs	healthy: 54.18 ± 8.62 MCD: 51.45 ± 7.27	healthy: 82.36 ± 6.02/136.54 ± 9.16 MCD: 87.1 ± 10.8/138.55 ± 13.03	walk, 0.65–1.1 m/s (treadmill)
Duerr et al. [63]	Different mid to large breed dogs	63.4 ± 7.7	82.1 ± 8.6/145.5 ± 10.8	trot, 2.4–2.5 m/s (overground)
Lorke et al. [64]	Beagle	young: 68.8 ± 2.7 old: 62.9 ± 5.1	young: 83.2/152.0 ± 10.5 old: 76.8/139.6 ± 12.4	trot, 1.7–1.8 m/s (treadmill)
Kopec et al. [65]	Different mid to large breed dogs	flat: 65.81 desc. Stair: 80.43 desc. Ramp: 67.95	66.23/132.03 34.36/114.79 46.0/113.95	walk, 1.01–1.45 m/s (overground & stair exercise)
Humphries et al. [66]	Labrador Retriever German Shepherd	left: 70.63 right: 67.13 left: 67.13 right: 67.94	77.21/147.84 77.21/144.34 75.45/142.58 74.37/142.31	trot, 2.19–2.45 m/s (walkway)
De Souza et al. [67]	American Pit Bull Terrier	walk: 45.22 trot: 52.39	walk: 111.25/167.65 trot: 110.14/163.00	walk, 1.17 ± 0.17 m/s trot, 2.04 ± 0.33 m/s (overground)

Table 2.
Summary of the values for range of motion in sagittal plane and flexion and extension angles of the canine elbow joint from different kinematic studies. All values are expressed in degrees and were calculated, if necessary, based on data of each study to allow comparison between studies. 180 degrees represent maximum extension and 0 degrees maximum flexion.

The stance phase is mainly characterized by continuous extension of the elbow joint until lifting of the paw from the ground. Some studies have shown flexion of the elbow joint just after weight bearing [43, 45, 47, 53, 58, 60, 64], resulting in two peaks of extension during the gait cycle. The first peak of extension occurs during the late swing phase and the initiation of ground contact and a second peak occurs at the end of the stance phase. The amount of this flexion differs between studies by several degrees. Further, this movement has not been described using fluoroscopic kinematography, what represents the gold standard of kinematic gait analysis [28]. This might be due to breed and inter-individual differences in the gait, due to the different techniques used for kinematic analysis or due to a soft tissue artifact, which occurs with skin mounted markers, and does not represent the in vivo motion of the bony cubital joint, but the movement pattern of the complete limb including the soft tissues [28, 32, 33]. Maximum extension of the elbow joint is reached at the end of the stance phase and is followed by continuous flexion during the swing phase. The peak flexion of the elbow joint is reached at approximately the middle of the swing phase and is followed by continuous extension of the elbow joint as a preparation for paw strike [53, 60, 64].

Besides flexion and extension, which represent the main motion pattern of the elbow joint, supination and pronation of the antebrachium and abduction and adduction of the humerus and antebrachium occur during the regular locomotion. In healthy Labrador retrievers the antebrachium is positioned in mild supination at the initial stance phase and shows minimal pronation during the remainder stance phase with a mean supination of the antebrachium of 3 ± 9 degrees [60]. In healthy Beagle the forelimb is placed onto the ground in mild pronation and is kept in this position during two thirds of the stance phase and then externally rotated during the last third of stance [28]. During the initial swing phase the antebrachium is supinated and maximum supination (mean 19 ± 9 degrees) occurs at the middle of the swing phase, together with maximum flexion of the elbow joint, in healthy Labrador retrievers [60]. In orthopedic sound Beagle a similar motion pattern is present during the swing phase, with supination of the antebrachium occurring during the first third of the swing phase [28]. Prior to foot strike rapid pronation of the antebrachium occurs and the limb is placed on the ground in a slightly supinated position in Labrador retrievers and slight pronation in Beagle [28, 60].

Three dimensional micromotion of the humerus, radius and ulna relative to each other was measured in different studies using marker based fluoroscopic kinematographic analysis [22–24, 54, 72]. Results of these studies show that the bones of the antebrachium have a complex motion pattern and radius and ulna cannot be seen as one single object. At the walk and the trot an axial movement between radius and ulna occurs in healthy and MCD affected elbows [22, 54]. In healthy canine elbow joints the radius shows an mean axial movement of 0.7 (SD 0.31) mm to 0.8 mm in relation to the ulna. This axial motion was detected in different mid to large breed dogs, like Fox hounds, Australian shepherd, Labrador retriever, Eurasian, German shepherd, Bernese mountain dog and mixed breeds [22, 54]. After the initiation of ground contact the radius moves proximally and remains in a slightly elevated position relative to the ulna, resulting in a dynamic negative radio-ulnar incongruence (RUI) [22, 72]. These results correspond with data from an in vitro study, which investigated the effects of limb loading and flexion and extension onto the radio-ulnar joint conformation and intra articular contact areas and which showed, that elbow extension leads to a relative lowering of the ulna in relation to the radius [73]. Extension is the main

motion of the elbow during the weight bearing phase and therefore the induction of a dynamic negative RUI might be seen as a adaption to joint loading [72]. Further, internal and external rotation between the radius and ulna occurs during the walk. Prior to foot strike the radius is in an externally rotated position relative to the ulna und shows internal rotation during the first third of the stance phase. Mean range of motion of the in vivo internal-external radial rotation is 11.4 (SD 2.0) degrees during the initial weight bearing phase [74]. No data exist investigating the in vivo radio-ulnar movement during the later stance phase and the swing. Therefore, the in vivo motion of the antebrachial bones and the dynamic changes within the radio-ulnar joint during the complete gait cycle are still unknown.

The in vivo humero-ulnar micromotion has only been investigated in one study so far [23]. Movement between the humerus and the ulna is characterized by flexion and extension, but rotational movement of the humerus relative to the ulna takes also place during locomotion [23]. At the walk the humerus shows an relative external rotation of 2.9 (SD 1.1) degrees during the first third of the stance phase in healthy humero-ulnar joints [23, 28]. These data imply that the elbow joint is not completely restricted to sagittal motion only. One study, investigating the 3D kinematics of the whole canine forelimb showed, that at the moment of ground contact the humerus is in an internally rotated position, which is slightly less at the trot compared to the walk (mean segment angle, walk: −34 degrees; trot: −25 degrees) [28]. During the walk the humerus shows internal and external rotation and only external rotation during the trot throughout the complete stance and swing phase, with a net external rotational movement during the stance phase [28]. This external rotational motion of the humerus is contrary to the internal rotation (pronation) of the antebrachium, which occurs prior to paw strike and is maintained during the stance [28, 60].

3.3 The dysplastic elbow joint

When kinematics of the diseased canine elbow joint are evaluated two different types of changes in the kinematic pattern have to be differentiated. First, changes attributed to pain and lameness, i.e. altered kinematics as a result of the disease. Second, changes in elbow joint kinematics, which represent a causative factor of the disease process.

Due to pain, caused by different joint pathologies in the elbow with DED, multiple adaptive mechanisms occur in the affected forelimb. Decreases in stance time, angular displacement and net joint moments can all be seen in the diseased elbow joint [51].

A reduced range of motion in the sagittal plane (flexion-extension) is present in dogs with MCD [51, 59, 60]. In particular flexion of the joint is decreased and the elbow kept in a more extended position during the gait. In Labrador retrievers with MCD a faster extension of the cubital joint occurs during late swing phase and the elbow is more extended by 9 degrees (mean) during initial ground contact and the early stance phase compared to orthopedically healthy elbows [60]. This more extended gait is a compensating mechanism and aims to reduce pressure at the medial joint compartment [7, 73, 75]. At the end of the stance and beginning of swing phase the elbow joint is more rapidly flexed in affected dogs. However, no active push off occurs at the end of the stance phase indicating that the affected limb is pulled off the ground by the proximal musculature [51]. Reduction in active push off aims to reduce the pressure acting on the joint surface. The elbow is held 16 degrees more externally rotated during the end of swing and initial stance phase and the antebrachium is

in average 2 degrees more abducted throughout the gait cycle and 9 degrees more supinated during the paw strike and early stance phase [60]. These changes have to be assumed as compensating mechanisms as well. Supination leads to caudal displacement of the peak pressure at the medial ulnar joint surface and by that to a release of pressure and potentially pain at the diseased medial coronoid process. Besides the Labrador retriever a more extended elbow joint is present in other breeds with MCD, e.g. Rottweiler, Staffordshire Bullterrier, Airdale terrier, Golden retriever, Polish Lowland sheepdog, German wirehaired pointer, Belgian malinois, Irish setter and mixed breed dogs [51, 59, 60]. Therefore, these changes in the kinematic pattern represent a general secondary adaption to intra articular pathologies and the corresponding pain in canine elbow joints with MCD.

Primary changes in the kinematics of the radius, ulna and humerus are assumed to play an role in the pathogenesis of MCD. Altered kinematics in the proximal radio-ulnar joint, were suggested by different researchers to be one potential factor influencing the development of MCD [76–90]. One proposed mechanism was an increased axial translation of the radius relative to the ulna leading to an dynamic radio-ulnar incongruence. Translational movement between the radius and ulna occurs in elbows with and without MCD in vivo [22, 54], with no significant difference in the total amount of movement between both groups [22]. Therefore, increased axial movement between the radius and ulna and induction of a dynamic RUI under weight bearing conditions could be excluded as an primary factor. However, the direction of radial motion is different between normal and diseased joints, with a negative RUI being induced during the initial stance phase in healthy elbows and no significant change in the radio-ulnar joint conformation in MCD affected joints [72]. Based on the results of that study dogs with a static RUI are not able to compensate the radio-ulnar step formation by radio-ulnar translation and dogs with MCD, but without a static RUI, do not show the same amount of negative dynamic RUI as measured in healthy canine elbow joints [72]. The induction of a negative radio-ulnar step during weight bearing might be a protective mechanism in healthy canine elbow joints. Lowering of the ulna or elevation of the radius during extension of the elbow joint was previously described in vitro and leads to a decrease of intra articular pressure at the medial joint compartment [73]. The inability of the diseased canine elbow joint to adjust the radio-ulnar joint conformation during loading might be one potential biomechanical factor in the pathogenesis of MCD. Especially in dogs without a measurable static incongruence, which account for 40% of all patients with MCD [76], the insufficient adaption to intra articular joint loads can lead to mechanical overload at one distinct joint compartment. Increased radio-ulnar rotation was proposed as another potential cause of mechanical overload along the radial incisure of the medial coronoid process and subsequent cartilage and bone damage [82, 87–90]. The only study comparing in vivo radio-ulnar rotational movement in healthy joints to joints with MCD showed no significant difference in the total amount of radial rotation and in the motion pattern of the radius [74]. The radius starts in an externally rotated position during the late swing phase just before paw strike and rotates internally in relation to the ulna during the early weight bearing phase. At approximately 30 to 40% of the stance phase the radius shows an external rotation again. Values of total rotational movement and internal/external movement of the radius show no significant difference between normal and affected elbow (internal radial rotation, healthy: 5.7 [SD 2.1] degrees; MCD: 5.3 [SD 2.6] degrees; $p = 0.1727$; external radial rotation, healthy: - 5.8 [SD: 1.3] degrees; MCD: - 4.5 [1.7] degrees; $p = 0.7705$; total rotation, healthy: 11.4 [SD: 2.0] degrees; MCD: 9.8 [SD: 3.2]; $p = 0.2904$) [74]. Absence of
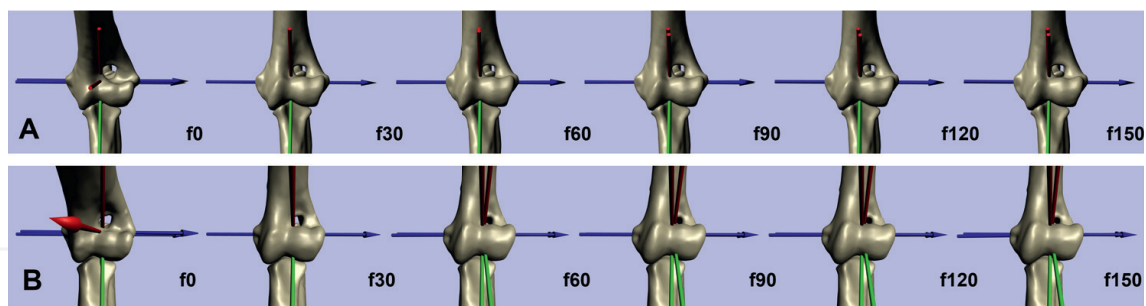
Figure 1.
Image sequence of the in vivo humero-ulnar joint motion during the late swing phase (f0), at the moment of weight bearing (f30) and the first third of the stance phase (f60 – f150). (A) Healthy joint; (B) MCD affected joint; relative external rotation of the humerus occurs just after ground contact, when the joint gets loaded. External rotation of the condyle leads to a craniolateral shift of the trochlea, impinging on the lateral aspect of the medial coronoid process [23].

increased radio-ulnar rotational motion does not exclude an biomechanical overload along the lateral aspect of the medial coronoid process of the ulna caused by interaction with the radial head. An abaxial attachment of the tendon of the biceps brachii muscle at the ulna was detected in dogs with MCD [90]. The pull of the biceps brachii muscle on the ulna could potentially lead to increased pressure between the medial coronoid and the radial head without altering the kinematics. However, no studies have investigated the forces acting between radius and ulna and compared these data between healthy and MCD affected dogs.

Another significant difference can be seen in the humero-ulnar rotational movement between healthy and MCD affected joints. Increased external rotation of the humeral condyle in relation to the ulna occurs at the first third of the stance phase in cubital joints with MCD (humeral rotation, healthy: 2.9 [SD 1.1] degrees; MCD: 5.3 [SD 2.0] degrees; p = 0.0229) [23]. This rotation of the humeral condyle leads to compression of the joint space between the medial coronoid process and the humeral trochlea, and might potentially lead to mechanical overload at the coronoid process and consequently to cartilage and subchondral bone damage (**Figure 1**). Therefore, increased humero-ulnar rotation has to be considered as one dynamic factor in the pathogenesis of MCD. If this increased humero-ulnar rotational movement is caused by soft tissue laxity, like in the dysplastic hip joint, altered muscle function or due to bony differences altering the joint function has not been investigated so far. The influence of a static positive radio-ulnar incongruence onto the contact areas and pressure distribution within the humero-ulnar joint is known [91–93]. However, the literature is lacking kinematic analysis investigating the influence of a static RUI on elbow joint motion, particular the humero-radio-ulnar micromotion. In the cited study on humero-ulnar kinematics the MCD group consisted of dogs with and without a static positive RUI [23]. Due to the small sample size no correlation could be found between the presence of static RUI and the amount of humeral rotational motion. Therefore, the influence of this significant bony deformity on the kinematics of the elbow joint remains unknown.

4. Joint contact areas and force distribution within the elbow joint

The mean body weight distribution between fore- and hindlimbs is approximately 60% : 40% in dogs [56, 94]. A large study investigating 123 different breeds found

that the grand mean proportion of mass was 60.4% on the forelimbs (range: 47.6 to 74.4%) [94]. Only sex was shown to be a significant factor altering that ratio, with females being below the mean value throughout different breeds [94]. Another study comparing kinematic and kinetic data of orthopedic healthy Labrador retrievers and German shepherds reported that Labrador retrievers carry a higher percentage of the weight on their forelimbs compared to the German shepherd (69% vs. 62%, p < 0.001) [66]. If this breed specific mechanical overload plays a role in the pathogenesis of DED and contributes to the high rate of Labrador retrievers with developmental elbow disease, in particular MCD, is not known.

Within the elbow joint load and forces are not homogenously distributed throughout the whole joint surface. It was believed that the radial joint surface is the main weight bearing surface of the radio-ulnar joint. However, more recent studies have shown, that the radius takes 51 to 52% of load [73, 75, 91]. Therefore the ulna plays a more important role in weight bearing than previously assumed. Despite an overall equal load and force distribution between the radius and the ulna, not every part of the joint surface represents an active joint contact area. Within the combined radio-ulnar joint surface three distinct contact areas can be found: the craniolateral aspect of anconeal process, the joint surface of the radial head, and the medial coronoid process [7, 24, 73]. There is no particular contact at the medial aspect of the anconeal process and the center of the trochlear notch (**Figure 2**). The latter one might be explained by the slight physiological humero-ulnar incongruence leading to a bicentrical contact
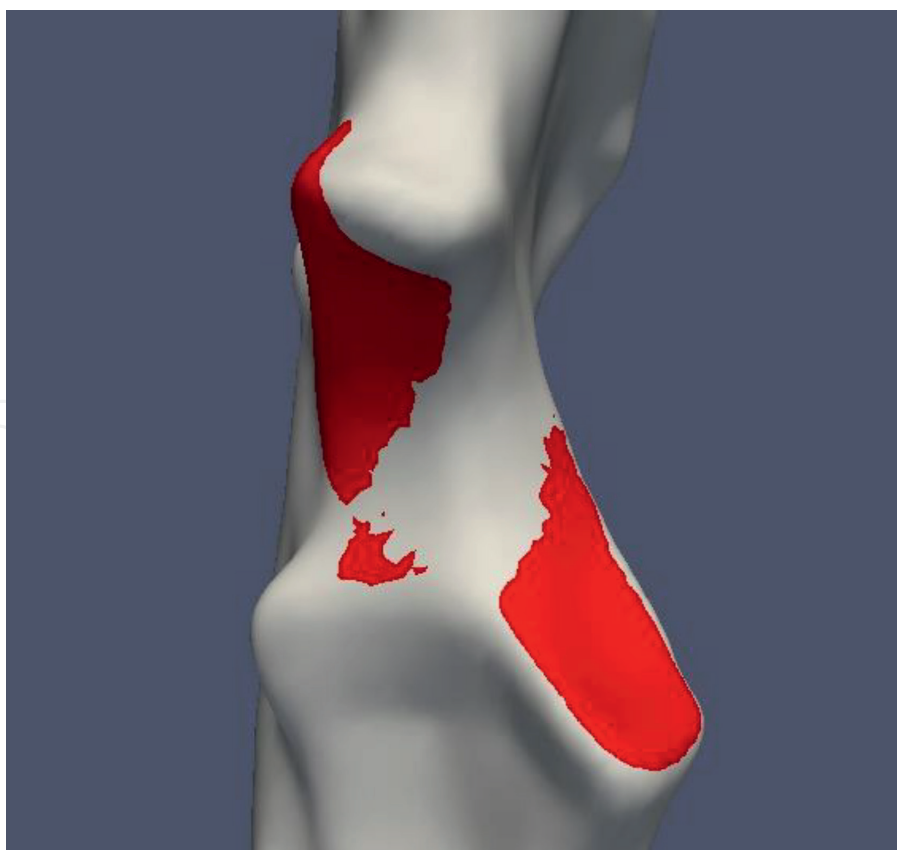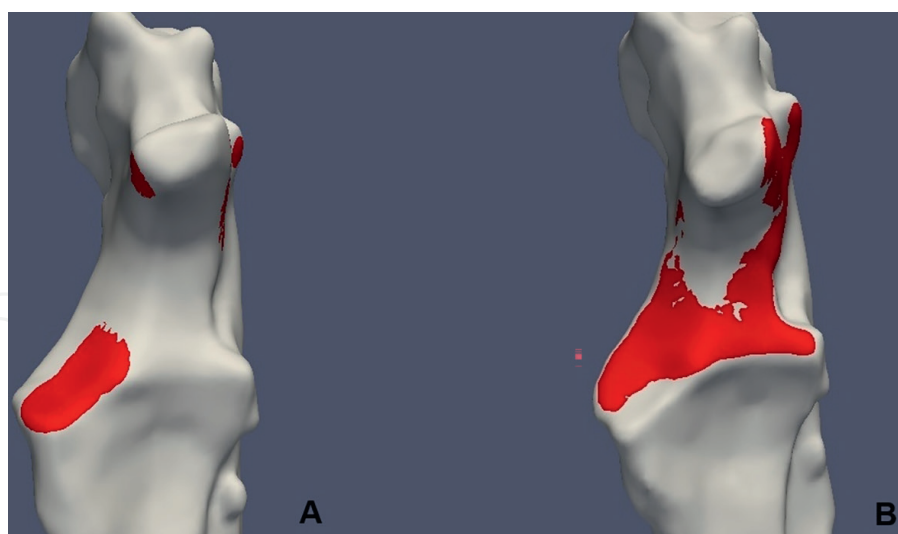

Figure 2.
Colored animation of the in vivo humero-ulnar joint contact pattern at the ulnar joint surface at the beginning of weight bearing in a healthy canine elbow joint (red: Humero-ulnar contact). Joint contact is present along the medial coronoid process and the lateral and proximal aspect of the trochlear notch. The radius is not shown in this animation.

pattern [6, 7, 9, 73, 95]. When the elbow joint is loaded the force applied by the humeral condyle is distributed along the anconeal process and the coronoid region. With increasing load the concave ulnar notch is stretched and these pressure forces are partially transformed to traction forces [8, 95–97]. Therefore this physiological incongruence leads to a more even stress distribution within the humero-ulnar joint. In human elbow joints the proximal and distal contact area confluent when high loads are acting onto the ulnar joint surface [98]. This load dependent change in contact pattern has not been described in canine elbows so far [7].

The presence of these three contact areas within the elbow joint is further supported by increased subchondral bone density measurements at these anatomic areas [95, 99]. Bone is a dynamic tissue which has the ability to remodel in response to mechanical load (Wolff's law) [100]. Therefore, increased bone density can be found in areas with increased load. Increased subchondral bone densities are present at the disto-medial and cranial aspect of the humeral trochlea and in the olecranon fossa, the anconeal and medial coronoid processes of the ulna and the cranio-medial region of the joint surface of the radius [95]. The same study showed a significant age-dependent increase in the subchondral bone density of the joint surfaces of all three bones, representing continuous adaption of the bone to mechanical stress with increasing age [95].

Though increased loading of the ulnar joint surface does not result in confluence of the bicentric contact pattern, other factors can influence the joint contact patterns of the humero-ulnar and humero-radial joint surfaces. An in vitro study investigated the influence of positive radio-ulnar incongruence (short radius) on joint contact patterns. Presence of a positive RUI leads to a shift of the contact area at the medial coronoid process towards the cranio-lateral aspect of the coronoid process and reduction of the anconeal contact area [93]. Other in vitro studies show similar results. After induction of a 1.9 mm positive RUI medial compartment contact area decreases significantly while the lateral contact area increases. Likewise the mean contact pressure and peak contact pressure increase within the medial compartment and decrease in the lateral part [91, 92]. Therefore, presence of a static positive RUI has to be assumed as an important factor in the disease process of developmental elbow disease and a correlation between the severity of cartilage damage and static RUI has been shown in affected elbows [76, 77, 101]. In vivo evaluation of the ulnar joint contact pattern during the walk in a dog with positive static RUI before and after bi-oblique dynamic proximal ulnar osteotomy (DPUO) confirmed the results of different in vitro studies [24]. Following DPUO positive static RUI decreased, leading to a significant increase of the contact area at the medial coronoid process and to a shift of the contact area from the cranio-lateral aspect (tip and radial incisure) towards the medial aspect and the base of the medial coronoid process (**Figure 3**) [24]. This positive effect of different forms of ulnar and humeral osteotomies onto humero-radio-ulnar contact and force distribution has previously been shown in vitro [75, 91, 92]. Whether a static RUI changes the kinematic pattern of humero-radial, humero-ulnar or radio-ulnar motion and by that the intra articular contact areas and pressure distribution or has a purely mechanical influence without dynamic changes has not been investigated so far.

Further, joint contact areas change during the regular locomotion. Pronation leads to reduction of the contact area in the medial and to a lesser amount in the lateral compartment of the radio-ulnar joint surface. The effect of pronation is further influenced by the elbow joint angle, with significant reduction of the medial contact area by 23% at 135 degree of flexion, what represents the average flexion angle during

Figure 3.
Humero-ulnar joint contact pattern at the ulnar joint surface at the beginning of weight bearing in a canine elbow joint with MCD (red: Contact area). (A) Contact pattern before bi-oblique DPUO; focal concentration of joint contact at the medial coronoid process (MCP) and slight contact at the medial and lateral aspect of the anconeal process is present. (B) Contact pattern 12 weeks postoperative; joint contact is more homogenously distributed throughout the ulnar joint surface and the craniolateral aspect of the MCP is even not in contact with the corresponding humeral trochlea [24].

the stance phase [73]. A reduced contact area will result in increased pressure when the same load is applied to the joint. Further, pronation of the antebrachium leads to a shift of the peak contact pressure towards the apex of the medial coronoid process. Otherwise supination of the antebrachium leads to caudal displacement of the peak contact pressure on the medial coronoid process [73, 75]. This might explain that dogs with medial coronoid disease show a more supinated stance to release pressure from the apex of the medial coronoid [60]. Moreover, flexion and extension, the main motion pattern during the normal locomotion, influence the intra articular pressure distribution. Flexion increases peak pressure at the medial radio-ulnar joint compartment and extension decreases pressure [73]. It is assumed that this change is due to dynamic changes within the radio-ulnar joint surface in healthy canine elbows [72, 73]. In a cadaveric study extension of the elbow joint induced lowering of the radius and ulna, however more pronounced in the ulna (3.8 mm) compared to the radius (1.9 mm). This corresponds to findings of the in vivo investigation of the radio-ulnar joint cup conformation in healthy elbow joints during the walk, where a negative RUI (short ulna) was induced during weight bearing [72]. This lowering of the ulna relative to the radius might protect the medial coronoid process from mechanical overload during locomotion in healthy canine elbows. In contrast, altered radio-ulnar kinematics preventing elevation of the radius might lead to continuous excessive mechanical overload and subsequent joint pathologies.

Considering the changes of intra articular contact areas and pressure distribution as a function of limb position might explain the typical clinical signs in dogs with developmental elbow disease. Affected dogs stand with the elbow slightly abducted and the antebrachium in slight external rotation (supination) [102]. Furthermore, the elbow joint is more rapidly extended during the swing phase and kept in a more extended position during weight bearing [60]. This motion pattern aims to reduce the contact and pressure at the medial coronoid process, where most commonly lesions attributed to developmental elbow disease occur [90, 103].

5. Conclusion

Canine elbow joint kinematics are more complex than flexion and extension of the joint and influenced by multiple factors like breed, limb length, gait, exercise and joint pathologies. The precise interaction of the three joint forming bones is essential for physiologic joint contact and intra articular force and pressure distribution. Based on the current literature an significantly increased humero-ulnar rotational movement as well as an reduced adjustment of the radio-ulnar joint during the regular locomotion of the dog seem to be two essential pathological factors influencing the development of MCD. This kind of movement is only measurable using laborious techniques like 3D fluoroscopic based kinematography. Nevertheless, further studies are needed to evaluate the complex kinematics of the healthy and the diseased canine elbow joint and to understand the effect of different kinematics onto kinetics.

Conflict of interest

The author declares no conflict of interest.

Author details

Thomas Rohwedder
Small Animal Clinic, Freie University Berlin, Berlin, Germany

*Address all correspondence to: thomas.rohwedder@fu-berlin.de

IntechOpen

References

[1] Nickel R, Schummer A, Seiferle E. Lehrbuch der Anatomie der Haustiere. 8. ed. Stuttgart: Enke Verlag Parey; 2003.

[2] Constantinescu GM, Constantinescu IA. A clinically oriented comprehensive pictorial review of canine elbow anatomy. Vet Surg. 2009;38(2):135-143.

[3] Alves-Pimenta S, Colaco B, Fernandes AM, Goncalves L, Colaco J, Melo-Pinto P, et al. Radiographic assessment of humeroulnar congruity in a medium and a large breed of dog. Vet Radiol Ultrasound. 2017;58(6): 627-633.

[4] Alves-Pimenta S, Ginja MM, Fernandes AM, Ferreira AJ, Melo-Pinto P, Colaco B. Computed tomography and radiographic assessment of congruity between the ulnar trochlear notch and humeral trochlea in large breed dogs. Vet Comp Orthop Traumatol. 2017;30(1): 8-14.

[5] Collins KE, Cross AR, Lewis DD, Zapata JL, Goett SD, Newell SM, et al. Comparison of the radius of curvature of the ulnar trochlear notch of Rottweilers and Greyhounds. American journal of veterinary research. 2001;62(6): 968-973.

[6] Maierl J, Hecht S, Böttcher P, Matis U, Liebich HG, editors. New aspects of the functional anatomy of the canine elbow joint. 10th European Society of Veterinary Orthopaedics and Traumatology (ESVOT); 2000 2000 March 24-26; Munich, Germany.

[7] Preston CA, Schulz KS, Kass PH. In vitro determination of contact areas in the normal elbow joint of dogs. American journal of veterinary research. 2000;61(10):1315-1321.

[8] Alves-Pimenta S, Ginja MM, Colaco B. Role of Elbow Incongruity in Canine Elbow Dysplasia: Advances in Diagnostics and Biomechanics. Vet Comp Orthop Traumatol. 2019;32(2):87-96.

[9] Eckstein F, Löhe F, Schulte E, Müller-Gerbl M, Milz S, Putz R. Physiological incongruity of the humero-ulnar joint: a functional principle of optimized stress distribution acting upon articulating surfaces? Anat Embryol. 1993;188:449-455.

[10] Brunnberg L, Waibl H, Lehmann J. Lahmheit beim Hund. 1. ed. Berlin: Procane Claudo; 2014.

[11] Clarke E, Aulakh KS, Hudson C, Barnes K, Gines JA, Liu CC, et al. Effect of sedation or general anesthesia on elbow goniometry and thoracic limb circumference measurements in dogs with naturally occurring elbow osteoarthritis. Vet Surg. 2020;49(7): 1428-1436.

[12] Formenton MR, de Lima LG, Vassalo FG, Joaquim JGF, Rosseto LP, Fantoni DT. Goniometric Assessment in French Bulldogs. Front Vet Sci. 2019;6:424.

[13] Thomas TM, Marcellin-Little DJ, Roe SC, Lascelles BDX, Brosey BP. Comparison of measurements obtained by use of an electrogoniometer and a universal plastic goniometer for the assessment of joint motion in dogs. American journal of veterinary research. 2006;67(12):1974-1979.

[14] Jaegger G, Marcellin-Little DJ, Levine D. Reliability of goniometry in Labrador Retrievers. American journal of veterinary research. 2002;63(7): 979-986.

[15] Farrell M, Draffan D, Gemmill T, Mellor D, Carmichael S. In vitro validation of a technique for assessment of canine and feline elbow joint collateral ligament integrity and description of a new method for collateral ligament prosthetic replacement. Vet Surg. 2007;36(6):548-556.

[16] Wakuri H, Kano Y. Anatomical studies on the brachioradial muscle in dogs. Acta Anat Nippon. 1966;41:22-31.

[17] Sandberg GS, Torres BT, Budsberg SC. Review of kinematic analysis in dogs. Vet Surg. 2020;49(6): 1088-1098.

[18] Geiger SM, Reich E, Böttcher P, Grund S, Hagen J. Validation of biplane high-speed fluoroscopy combined with two different noninvasive tracking methodologies for measuring in vivo distal limb kinematics of the horse. Equine veterinary journal. 2018;50(2): 261-269.

[19] Brainerd EL, Baier DB, Gatesy SM, Hedrick TL, Metzger KA, Gilbert SL, et al. X-ray reconstruction of moving morphology (XROMM): precision, accuracy and applications in comparative biomechanics research. J Exp Zool A Ecol Genet Physiol. 2010;313(5):262-279.

[20] Miranda DL, Schwartz JB, Loomis AC, Brainerd EL, Fleming BC, Crisco JJ. Static and Dynamic Error of a Biplanar Videoradiography System Using Marker-Based and Markerless Tracking Techniques. J Biomech Eng. 2011;133(12): 121002-121010.

[21] Fischer MS, Lehmann SV, Andrada E. Three-dimensional kinematics of canine hind limbs: in vivo, biplanar, high-frequency fluoroscopic analysis of four breeds during walking and trotting. Sci Rep. 2018;8(1):16982.

[22] Rohwedder T, Fischer M, Böttcher P. In-vivo fluoroscopic kinematography of dynamic radio-ulnar incongruence in dogs. Open Veterinary Journal. 2017; 7(3):221-228.

[23] Rohwedder T, Fischer M, Böttcher P. In vivo axial humero-ulnar rotation in normal and dysplastic canine elbow joints. Tierarztliche Praxis Ausgabe K, Kleintiere/Heimtiere. 2018;46(2):83-89.

[24] Rohwedder T, Rebentrost P, Böttcher P. Three-Dimensional Joint Kinematics in a Canine Elbow Joint with Medial Coronoid Disease before and after Bi-Oblique Dynamic Proximal Ulnar Osteotomy. VCOT Open. 2019;02(02):e44-ee9.

[25] Tashman S, Andrest W. In-vivo measurement of dynamic joint motion using high speed biplane radiography and CT: application to canine ACL deficiency. J Biomech Eng. 2003;125(2): 238-245.

[26] Tashman S, Anderst W, Kolowich P, Havstad S, Arnoczky SP. Kinematics of the ACL-deficient canine knee during gait: serial changes over two years. J Orthop Res. 2004;22(5):931-941.

[27] Korvick DL, Pijanowski GJ, Schaeffer DJ. Three-dimensional kinematics of the intact and cranial cruciate ligament-deficient stifle of dogs. Journal of biomechanics. 1994; 27(1):77-87.

[28] Andrada E, Reinhardt L, Lucas K, Fischer MS. Three-dimensional inverse dynamics of the forelimb of Beagles at a walk and trot. American journal of veterinary research. 2017;78(7): 804-817.

[29] Kim SE, Jones SC, Lewis DD, Banks SA, Conrad BP, Tremolada G, et al.

In-vivo three-dimensional knee kinematics during daily activities in dogs. J Orthop Res. 2015;33(11):1603-1610.

[30] Rey J, Fischer MS, Böttcher P. Sagittal joint instability in the cranial cruciate ligament insufficient canine stifle. Caudal slippage of the femur and not cranial tibial subluxation. Tierarztliche Praxis Ausgabe K, Kleintiere/Heimtiere. 2014;42(3):151-156.

[31] Bauman JM, Chang YH. High-speed X-ray video demonstrates significant skin movement errors with standard optical kinematics during rat locomotion. J Neurosci Methods. 2010;186(1):18-24.

[32] Kim SY, Kim JY, Hayashi K, Kapatkin AS. Skin movement during the kinematic analysis of the canine pelvic limb. Vet Comp Orthop Traumatol. 2011;24(5):326-332.

[33] Schwencke M, Smolders LA, Bergknut N, Gustas P, Meij BP, Hazewinkel HA. Soft tissue artifact in canine kinematic gait analysis. Vet Surg. 2012;41(7):829-837.

[34] Torres BT, Whitlock D, Reynolds LR, Fu YC, Navik JA, Speas AL, et al. The effect of marker location variability on noninvasive canine stifle kinematics. Vet Surg. 2011;40(6):715-719.

[35] Torres BT, Punke JP, Fu YC, Navik JA, Speas AL, Sornborger A, et al. Comparison of canine stifle kinematic data collected with three different targeting models. Vet Surg. 2010;39(4): 504-512.

[36] Gatesy SM, Baier DB, Jenkins FA, Dial KP. Scientific rotoscoping: a morphology-based method of 3-D motion analysis and visualization. J Exp Zool A Ecol Genet Physiol. 2010; 313(5):244-261.

[37] Anderst W, Zauel R, Bishop J, Demps E, Tashman S. Validation of three-dimensional model-based tibio-femoral tracking during running. Med Eng Phys. 2009;31(1):10-16.

[38] Anderst WJ, Baillargeon E, Donaldson WF, 3rd, Lee JY, Kang JD. Validation of a noninvasive technique to precisely measure in vivo three-dimensional cervical spine movement. Spine (Phila Pa 1976). 2011;36(6): E393-E400.

[39] Giphart JE, Zirker CA, Myers CA, Pennington WW, LaPrade RF. Accuracy of a contour-based biplane fluoroscopy technique for tracking knee joint kinematics of different speeds. Journal of biomechanics. 2012;45(16):2935-2938.

[40] Li G, Van de Velde SK, Bingham JT. Validation of a non-invasive fluoroscopic imaging technique for the measurement of dynamic knee joint motion. Journal of biomechanics. 2008;41(7):1616-1622.

[41] Lin H, Wang S, Tsai TY, Li G, Kwon YM. In-vitro validation of a non-invasive dual fluoroscopic imaging technique for measurement of the hip kinematics. Med Eng Phys. 2012;35(3):411-416.

[42] Bey MJ, Zauel R, Brock SK, Tashman S. Validation of a new model-based tracking technique for measuring three-dimensional, in vivo glenohumeral joint kinematics. J Biomech Eng. 2006;128(4):604-609.

[43] DeCamp CE, Soutas-Little RW, Hauptman J, Olivier B, Braden T, A. W. Kinematic gait analysis of the trot in healthy greyhounds. American journal of veterinary research. 1993;54(4):627-634.

[44] Allen K, DeCamp CE, Braden TD, Balms M. Kinematic Gait Analysis of the

Trot in Healthy Mixed Breed Dogs. Vet Comp Orthop Traumatol. 1994;7(4): 148-153.

[45] Hottinger HA, DeCamp CE, Olivier B, Hauptman JG, Soutas-Little RW. Noninvasive kinematic analysis of the walk in healthy large-breed dogs. American journal of veterinary research. 1996;57(3):381-389.

[46] Gillette R, Zebas CJ. A Two-Dimensional Analysis of Limb Symmetry in the Trot of Labrador Retrievers. J Am Anim Hosp Assoc. 1999;35(6):515-20.

[47] Nielsen C, Stover SM, Schulz KS, Hubbard M, Hawkins DA. Two-dimensional link-segment model of the forelimb of dogs at a walk. American journal of veterinary research. 2003; 64(5):609-617.

[48] Owen MR, Richards J, Clements DN, Drew ST, Bennett D, Carmichael S. Kinematics of the elbow and stifle joints in greyhounds during treadmill trotting – An investigation of familiarisation. Vet Comp Orthop Traumatol. 2004;17(3): 141-145.

[49] Clements DN, Owen MR, Carmichael S, Reid SWJ. Kinematic analysis of the gait of 10 labrador retrievers during treadmill locomotion. Vet Rec. 2005;156(15):478-481.

[50] Feeney LC, Lin C, Marcellin-Little DJ, Tate AR, Queen RM, Yu B. Validation of two-dimensional kinematic analysis of walk and sit-to-stand motions in dogs. American journal of veterinary research. 2007;68(3):277-282.

[51] Burton NJ, Dobney JA, Owen MR, Colborne GR. Joint angle, moment and power compensations in dogs with fragmented medial coronoid process. Vet Comp Orthop Traumatol. 2008;21(2): 110-118.

[52] Holler PJ, Brazda V, Dal-Bianco B, Lewy E, Mueller MC, Peham C, et al. Kinematic motion analysis of the joints of the forelimbs and hind limbs of dogs during walking exercise regimens. American journal of veterinary research. 2010;71(7):734-740.

[53] Agostinho FS, Rahal SC, Miqueleto NS, Verdugo MR, Inamassu LR, El-Warrak AO. Kinematic analysis of Labrador Retrievers and Rottweilers trotting on a treadmill. Vet Comp Orthop Traumatol. 2011;24(3): 185-191.

[54] Guillou RP, Déjardin LM, Bey MJ, McDonald CP. Three Dimensional Kinematics of the Normal Canine Elbow at the Walk and Trot. 2011 American College of Veterinary Surgeons Veterinary Symposium November 3-5, Chicago, Illinois. Veterinary Surgery. 2011;40(7):E17-E42.

[55] Angle T, Gillette R, Weimar W. Kinematic analysis of maximal movement initiation in Greyhounds. Aust Vet J. 2012;90(3):60-68.

[56] Jarvis SL, Worley DR, Hogy SM, Hill AE, Haussler KK, Reiser RF. Kinematic and kinetic analysis of dogs during trotting after amputation of a thoracic limb. American journal of veterinary research. 2013;74(9): 1155-1163.

[57] Brady RB, Sidiropoulos AN, Bennett HJ, Rider PM, J. M-LD, P. D. Evaluation of gait-related variables in lean and obese dogs at a trot. American journal of veterinary research. 2013; 74(5):757-762.

[58] Miqueleto NS, Rahal SC, Agostinho FS, Siqueira EG, Araujo FA, El-Warrak AO. Kinematic analysis in healthy and hip-dysplastic German Shepherd dogs. Veterinary journal

(London, England : 1997). 2013;195(2):210-5.

[59] Galindo-Zamora V, Dziallas P, Wolf DC, Kramer S, Abdelhadi J, Lucas K, et al. Evaluation of thoracic limb loads, elbow movement, and morphology in dogs before and after arthroscopic management of unilateral medial coronoid process disease. Vet Surg. 2014;43(7):819-828.

[60] Caron A, Caley A, Farrell M, Fitzpatrick N. Kinematic gait analysis of the canine thoracic limb using a six degrees of freedom marker set. Study in normal Labrador Retrievers and Labrador Retrievers with medial coronoid process disease. Vet Comp Orthop Traumatol. 2014;27(6):461-469.

[61] Fischer MS, Lilje KE. Dogs in motion. 2nd ed. Dortmund: VDH Service GmbH; 2011.

[62] Catavitello G, Ivanenko YP, Lacquaniti F. Planar Covariation of Hindlimb and Forelimb Elevation Angles during Terrestrial and Aquatic Locomotion of Dogs. PLoS One. 2015;10(7):e0133936.

[63] Duerr FM, Pauls A, Kawcak C, Haussler K, Bertocci G, Moorman V, et al. Evaluation of inertial measurement units as a novel method for kinematic gait evaluation in dogs. Vet Comp Orthop Traumatol. 2016;29(6):475-483.

[64] Lorke M, Willen M, Lucas K, Beyerbach M, Wefstaedt P, Murua Escobar H, et al. Comparative kinematic gait analysis in young and old Beagle dogs. J Vet Sci. 2017;18(4):521-530.

[65] Kopec NL, Williams JM, Tabor GF. Kinematic analysis of the thoracic limb of healthy dogs during descending stair and ramp exercises. American journal of veterinary research. 2018;79(1):33-41.

[66] Humphries A, Shaheen AF, Gomez Alvarez CB. Biomechanical comparison of standing posture and during trot between German shepherd and Labrador retriever dogs. PLoS One. 2020;15(10): e0239832.

[67] de Souza MC, Calesso JR, Cenci B, Cardoso MJL, Moura FA, Fagnani R. Kinematics of healthy American Pit Bull Terrier dogs. Veterinární Medicína. 2021;66(No. 1):8-16.

[68] Gustas P, Pettersson K, Honkavaara S, Lagerstedt AS, Bystrom A. Kinematic and temporospatial assessment of habituation of Labrador retrievers to treadmill trotting. Veterinary journal (London, England : 1997). 2013;198 Suppl 1:e114-9.

[69] Gustas P, Pettersson K, Honkavaara S, Lagerstedt AS, Bystrom A. Kinematic and spatiotemporal assessment of habituation to treadmill walking in Labrador retrievers. Acta Vet Scand. 2016;58(1):87.

[70] Tian W, Cong Q, Menon C. Investigation on walking and pacing stability of german Shepherd dog for different locomotion speeds. J Bionic Eng. 2011;8(1):18-24.

[71] Colborne GR, Walker AM, Tattersall AJ, Fuller CJ. Effect of trotting velocity on work patterns of the hind limbs of Greyhounds. American journal of veterinary research. 2006;67(8): 1293-1298.

[72] Rohwedder T, Böttcher P. In vivo changes of the radio-ulnar joint conformation in canine elbow joints with and without medial coronoid process disease. 5th World Veterinary Orthopaedic Congress (WVOC); 2018 2018 September 12-15; Barcelona, Spain.

[73] Cuddy LC, Lewis DD, Kim SE, Conrad BP, Banks SA, Horodyski M,

et al. Contact mechanics and three-dimensional alignment of normal dog elbows. Vet Surg. 2012;41(7):818-828.

[74] Rohwedder T, Böttcher P. In vivo rotational movement of the radius in healthy canine elbow joints and elbows with medial coronoid process disease. Virtual ESVOT Congress, 2021 May 5-8; 2021.

[75] Mason DR, Schulz KS, Fujita Y, Kass PH, Stover SM. Measurement of humeroradial and humeroulnar transarticular joint forces in the canine elbow joint after humeral wedge and humeral slide osteotomies. Vet Surg. 2008;37(1):63-70.

[76] Eljack H, Böttcher P. Relationship between axial radioulnar incongruence with cartilage damage in dogs with medial coronoid disease. Vet Surg. 2015;44(2):174-179.

[77] Kramer A, Holsworth IG, Wisner ER, Kass PH, Schulz KS. Computed tomographic evaluation of canine radioulnar incongruence in vivo. Vet Surg. 2006;35(1):24-29.

[78] Krotscheck U, Böttcher P, Thompson MS, Todhunter RJ, Mohammed HO. Cubital subchondral joint space width and CT osteo-absorptiometry in dogs with and without fragmented medial coronoid process. Vet Surg. 2014;43(3):330-338.

[79] Smith TJ, Fitzpatrick N, Evans RB, Pead MJ. Measurement of Ulnar Subtrochlear Sclerosis Using a Percentage Scale in Labrador Retrievers with Minimal Radiographic Signs of Periarticular Osteophytosis. Veterinary Surgery. 2009;38(2):199-208.

[80] Starke A, Böttcher P, Pfeil I. [Radiologic quantification of the elbow conformation with a new method for acquiring standardized x-rays under load. Reference valus for medium sized and large dogs without dysplasia of the elbow joint]. Tierarztliche Praxis Ausgabe K, Kleintiere/Heimtiere. 2013;41(3):145-154.

[81] Starke A, Böttcher P, Pfeil I. [Comparative radiologic examination of the canine elbow with and without elbow dysplasia under standardized load]. Tierarztliche Praxis Ausgabe K, Kleintiere/Heimtiere. 2014;42(3): 141-150.

[82] Fitzpatrick N, Garcia TC, Daryani A, Bertran J, Watari S, Hayashi K. Micro-CT Structural Analysis of the Canine Medial Coronoid Disease. Vet Surg. 2016;45(3): 336-346.

[83] Fitzpatrick N, Smith TJ, Evans RB, O'Riordan J, Yeadon R. Subtotal coronoid ostectomy for treatment of medial coronoid disease in 263 dogs. Vet Surg. 2009;38(2):233-245.

[84] Fitzpatrick N, Yeadon R. Working algorithm for treatment decision making for developmental disease of the medial compartment of the elbow in dogs. Vet Surg. 2009;38(2):285-300.

[85] Gemmill TJ, Clements DN. Fragmented coronoid process in the dog: is there a role for incongruency? J Small Anim Pract. 2007;48(7):361-368.

[86] Might KR, Hanzlik KA, Case JB, Duncan CG, Egger EL, Rooney MB, et al. In Vitro Comparison of Proximal Ulnar Osteotomy and Distal Ulnar Osteotomy with Release of the Interosseous Ligament in a Canine Model. Veterinary Surgery. 2011;40(3):321-326.

[87] Baud K, Griffin S, Martinez-Taboada F, Burton NJ. CT evaluation of elbow congruity in dogs: radial incisure versus apical medial coronoid process

fragmentation. J Small Anim Pract. 2020;61(4):224-229.

[88] Burton NJ, Warren-Smith CM, Roper DP, Parsons KJ. CT assessment of the influence of dynamic loading on physiological incongruency of the canine elbow. J Small Anim Pract. 2013; 54(6):291-298.

[89] Hulse D, Young B, Beale B, Kowaleski M, Vannini R. Relationship of the biceps-brachialis complex to the medial coronoid process of the canine ulna. Vet Comp Orthop Traumatol. 2010;23(3):173-176.

[90] Veksins A, Kozinda O, Sandersen C. Computed tomographic morphometry of the biceps brachii muscle tendon of dogs affected by the medial coronoid disease. Anat Histol Embryol. 2019.

[91] Krotscheck U, Kalafut S, Meloni G, Thompson MS, Todhunter RJ, Mohammed HO, et al. Effect of Ulnar Ostectomy on Intra-Articular Pressure Mapping and Contact Mechanics of the Congruent and Incongruent Canine Elbow Ex Vivo. Vet Surg. 2014;43(3):339-346.

[92] McConkey MJ, Valenzano DM, Wei A, Li T, Thompson MS, Mohammed HO, et al. Effect of the Proximal Abducting Ulnar Osteotomy on Intra-Articular Pressure Distribution and Contact Mechanics of Congruent and Incongruent Canine Elbows Ex Vivo. Vet Surg. 2016;45(3):347-355.

[93] Preston CA, Schulz KS, Taylor KT, Kass PH, Hagan CE, Stover SM. In vitro experimental study of the effect of radial shortening and ulnar ostectomy on contact patterns in the elbow joint of dogs. American journal of veterinary research. 2001;62(10):1548-1556.

[94] Fish FE, Sheehan MJ, Adams DS, Tennett KA, Gough WT. A 60:40 split:

Differential mass support in dogs. Anat Rec (Hoboken). 2021;304(1):78-89.

[95] Dickomeit MJ, Böttcher P, Hecht S, Liebich HG, Maierl J. Topographic and age-dependent distribution of subchondral bone density in the elbow joints of clinically normal dogs. American journal of veterinary research. 2011;72(4):491-499.

[96] Eckstein F, Löhe F, Müller-Gerbl M, Steinlechner M, Putz R. Stress distribution in the trochlear notch. A model of bicentric load transmission through joints. The Journal of bone and joint surgery American volume. 1994; 76(4):647-653.

[97] Merz B, Eckstein F, Hillebrand S, Putz R. Mechanical implications of humero-ulnar incongruity – finite element analysis and experiment. Journal of biomechanics. 1997;30(7):713-721.

[98] Eckstein F, Löhe F, Hillebrand S, Bergmann M, Schulte E, Milz S, et al. Morphomechanics of the humero-ulnar joint: I. Joint space width and contact areas as a function of load and flexion angle. Anat Rec. 1995;243(3):318-326.

[99] Winhard FE. Anatomische und computertomographische Untersuchungen am gesunden und degenerativ veränderten Schulter- und Ellbogen- gelenk des Hundes (*Canis familiaris*) [Doctoral Thesis]. Munich: Ludwig- Maximilian-Universität München; 2007.

[100] Wolff J. The law of bone remodeling. 1 ed. Berlin Heidelberg: Springer-Verlag; 1986.

[101] Griffon DJ, Mostafa AA, Blond L, Schaeffer DJ. Radiographic, computed tomographic, and arthroscopic diagnosis of radioulnar incongruence in dogs with medial coronoid disease. Vet Surg. 2018; 47(3):333-342.

[102] Trostel CT, McLaughlin RM, Pool RR. Canine lameness caused by developmental orthopedic diseases. Compend Contin Educ Vet. 2003;25:112.

[103] Lavrijsen IC, Heuven HC, Voorhout G, Meij BP, Theyse LF, Leegwater PA, et al. Phenotypic and genetic evaluation of elbow dysplasia in Dutch Labrador Retrievers, Golden Retrievers, and Bernese Mountain dogs. Veterinary journal (London, England: 1997). 2012;193(2):486-92.